Simple method for balancing direct contact membrane distillation

Simple Method for Balancing Direct Contact Membrane Distillation [1]

Jaichander Swaminathan, Hyung Won Chung, David M. Warsinger, John H. Lienhard V [2]

Rohsenow Kendall Heat and Mass Transfer Laboratory, Department of Mechanical Engineering, Massachusetts Institute of Technology, Cambridge MA 02139-4307 USA

Abstract

A simple theoretical method for maximizing efficiency via real-time balancing of direct contact membrane distillation (DCMD) systems is presented. The method is applicable under variable operating conditions. Balancing involves measuring only the flow rates of feed stream out of the module and the cold water flow into the module, as well as the salinity of the feed. A valve or variable frequency drive is used to set the condensate water flow into the module so that the heat capacity rates of the hot and cold streams are equal. This method is much simpler and more general than what is proposed in the literature, which generally requires more measurements and a complicated expression. Balancing leads to 20-50% improvement in efficiency (GOR) compared to equal inflow of both feed and pure water streams, which is the common practice. Real-time balancing is particularly useful for variations in feed salinity, whereas the improvement by real-time balancing is low for changes in system top or bottom temperatures.

Keywords: Direct Contact Membrane Distillation, Real-time Balancing, Energy Efficiency, Flux, Desalination

[1] J. Swaminathan, H.W. Chung, D.M. Warsinger, J.H. Lienhard V, "Simple Method for Balancing Direct Contact Membrane Distillation," *Desalination*, Vol. 383, pp. 53–59, 1 April 2016, 10.1016/j.desal.2016.01.014

[2] Corresponding author: lienhard@mit.edu

Nomenclature

Roman Symbols

B	Membrane permeability, kg/m^2·s·Pa
BPE	Boiling Point Elevation, °C
c_p	Specific heat capacity, J/kg-K
d	Depth or thickness, m
DCMD	Direct Contact Membrane Distillation
GOR	Gained Output Ratio
h_fg	Enthalpy of vaporization, J/kg
HX	Heat exchanger
k	Thermal conductivity, W/m·K
L	Length of module, m
m	Molality, mol/kg
$\dot{m}$	Mass flow rate, kg/s
MD	Membrane Distillation
MR	Mass flow ratio of condensate stream to feed stream inflow
$\dot{Q}$	Heat transfer rate, W
p^vap	Vapor Pressure, Pa
s	Salt concentration, g/kg
T	Temperature, °C

Greek Symbols

δ	Membrane thickness, m
η	Thermal efficiency
ϕ	Porosity

Subscripts/Superscripts

amb	Ambient
c	Condensate
f	Feed
h	Heater
HX	Heat exchanger
in	Inlet
m	Membrane interface
out	Outlet
p	Product

1. Introduction

Membrane distillation (MD) systems are capable of treating highly concentrated water streams and are considered to be more fouling resistant than other membrane based desalination technologies [1]. MD can be configured as a single stage or a multi-stage system. In single stage MD, the pure water vapor leaving the membrane pores can either be condensed within the module or outside. MD configurations such as direct contact (DCMD) and air gap (AGMD) which involve condensation within the module have been found to be more suitable for achieving higher energy efficiency than systems like sweeping gas and vacuum MD with external condensation [2].

Thermal energy consumption constitutes the major portion of the cost of water from membrane distillation and for solar-driven MD systems energy efficiency governs the required capital investment in solar panels [3]. As a result, improving energy efficiency, measured here in the form of gained output ratio (or GOR), is of significant interest. While energy efficiency can be increased by increasing top temperature or system size, methods to increase energy efficiency without increasing capital cost, such as by optimizing system operating conditions are more advantageous:

$$\mathrm{GOR} = \frac{\dot{m}_{\mathrm{p}} h_{\mathrm{fg}}}{\dot{Q}_{\mathrm{h}}} \tag{1}$$

DCMD is the oldest configuration of MD and the most commonly studied configuration due to its relatively simple design [4]. Optimizing DCMD operation to improve energy efficiency is the focus of this work. In DCMD, hot saline water flows across one side of a microporous hydrophobic membrane. Cooler pure water is passed on the other side of the membrane. Due to the vapor pressure difference established by the temperature difference between the two streams, water vapor passes from the hot side to the cold side and condenses into the pure water stream. In addition, heat is also transferred from the hot side to the cold side in the form of conduction, which is a loss mechanism in MD. As a result of these two processes, the temperature of the hot stream decreases as it flows through the system and the temperature of the cold stream increases. In order to reuse energy and achieve gained output ratio (GOR) greater than 1, the energy in the warm distillate stream would have to be recovered. To do this, a counterflow external heat exchanger is used as shown in Fig. 1a that preheats the feed water before further heat is added in the feed top heater [5].

The pure water stream is recirculated after the fresh water produced within the MD module is removed. The feed may also be recirculated in a closed loop to increase the overall recovery ratio. Additional external cooling is necessary if both streams are recirculated, to prevent temperature rise of the feed and cold water loops. Heat recovery from the permeate stream can be achieved only when $T_{\mathrm{c,out}} > T_{\mathrm{f,out}}$ if the feed is recirculated. This condition may not be satisfied for very short length systems.

Some studies use an optional additional heat exchanger to reduce the pure water inflow temperature down to ambient temperature [6, 7]. This increases the temperature difference for desalination within the MD module, leading to higher flux. Figure 1b shows the difference in performance between using an additional heat exchanger and not using the additional heat exchanger based on numerical modeling. The system with an additional heat exchanger performs better especially when the MD area is small, and hence overall energy efficiency is low. For systems with larger membrane area, the difference in performance between the two systems is smaller. This computation was performed using the model described by Summers et al. [2], by setting $T_{\mathrm{c,in}} = T_{\mathrm{c,HX,out}}$ (for the case of no additional heat exchanger) or $T_{\mathrm{c,in}} = T_{\mathrm{amb}}$ (for the case of using a large additional HX). This study will focus on a system with no additional heat exchanger because of its relative simplicity and lower cost.

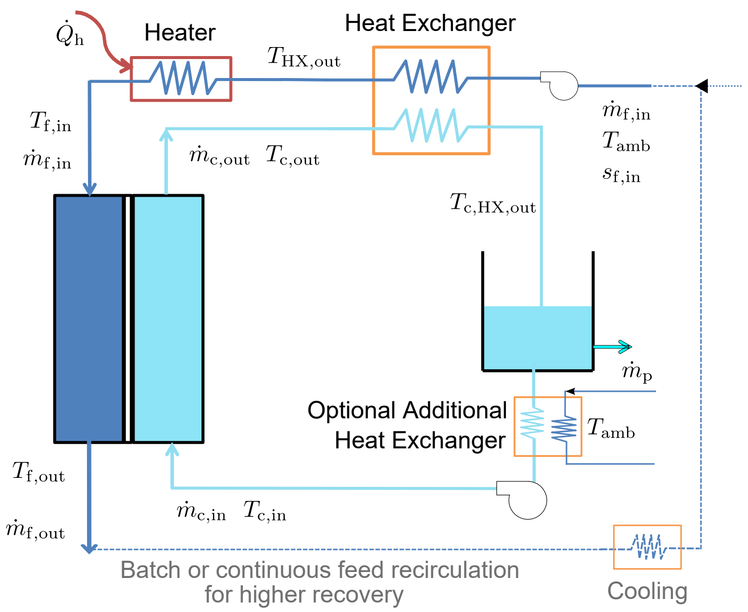

(a) Direct Contact Membrane Distillation process with a closed loop pure product.

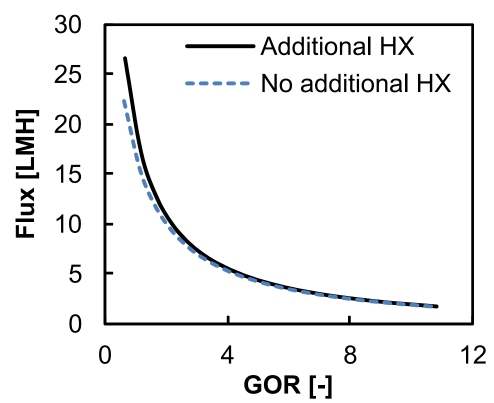

(b) Effect of additional cooling of condensate. Length is varied from 0.5 to 12 m. Other parameters are set at baseline values mentioned in Table 1.

Figure 1: DCMD system schematic diagram and effect of additional HX.

The hot and cold water streams are usually set up in counterflow configuration in order to distribute the flux uniformly within the system and achieve higher energy efficiency.

Swaminathan et al. [8] showed that the energy efficiency of permeate gap (PGMD) and conductive gap (CGMD) MD systems was maximized when the pure water in the gap flows countercurrent to the cold water stream, as opposed to parallel or crossflow conditions. When the pure water flows in the same direction as the hot stream and countercurrent to the cool stream, at any local position along the MD module, the total flow in either direction is equal. This leads to a more uniform driving temperature difference across the module length and higher energy efficiency by about 40% compared to a case with pure water flow co-current to the cold stream. Thermodynamically, this increased efficiency is attributed to lower specific entropy generation within the module.

Unlike in the case of AGMD and other configurations, in DCMD, the flow rate of the cold water stream can be varied independently of the warm water flow rate. Several studies in the past used an equal input flow rate of hot and cold water into the module. Guan et al. [7] performed DCMD simulations and found that the GOR was maximized when the feed and cold water inlet flow rates are approximately equal. Winter [9] experimentally showed that flux and GOR are both maximized under a symmetric operating condition where the mass flow rates of the hot and cold streams are equal at the hot end of the module.

Lin et al. [6] showed through numerical modeling of a coupled DCMD-Heat Exchanger (DCMD-HX) system, that the optimal value of cold pure water mass flow rate is not equal to that of the hot inflow, but about 90–92% of this value. They developed an analytical expression for this critical mass flow ratio, $\mathrm{MR}_{\mathrm{Lin}}$ as a function of T_{top}, T_{bottom}, $\mathrm{BPE}_{\mathrm{f,in}}$, $\mathrm{BPE}_{\mathrm{f,out}}$, $c_{\mathrm{p}}^{\mathrm{f}}$ and $c_{\mathrm{p}}^{\mathrm{c}}$ (Eq. 4) where mass flow rate ratio MR is defined as $\mathrm{MR} \equiv \frac{\dot{m}_{\mathrm{c,in}}}{\dot{m}_{\mathrm{f,in}}}$. Temperature and salinity are combined in the form of T^*, defined as:

$$T^*_{\mathrm{f,in}} = T_{\mathrm{sat}}\left(P_{\mathrm{vap}}\left(T_{\mathrm{f,in}}, s_{\mathrm{f}}\right)\right) \tag{2}$$

$$T^*_{\mathrm{c,in}} = T_{\mathrm{sat}}\left(P_{\mathrm{vap}}\left(T_{\mathrm{c,in}}, s_{\mathrm{f}}\right)\right) \tag{3}$$

where P_{vap} is the vapor pressure of salt water and is a function of temperature and salinity (s_{f}). A higher salinity results in a lower T^* through an increase in boiling point elevation (BPE), since $T^* \approx T - \mathrm{BPE}$.

The value of critical MR is then evaluated by considering the conditions for permeate limiting or feed limiting regime:

$$\mathrm{MR}_{\mathrm{Lin}} = \left(\frac{T_{\mathrm{f,in}} - T^*_{\mathrm{c,in}}}{T^*_{\mathrm{f,in}} - T_{\mathrm{c,in}}}\right) \cdot \left(\frac{\left(\frac{h_{\mathrm{fg}}}{c_{\mathrm{p}}^{\mathrm{c}}}\right) - \frac{T^*_{\mathrm{f,in}} - T_{\mathrm{c,in}}}{2}}{\left(\frac{h_{\mathrm{fg}}}{c_{\mathrm{p}}^{\mathrm{f}}}\right) + \left(\frac{c_{\mathrm{p}}^{\mathrm{c}}}{c_{\mathrm{p}}^{\mathrm{f}}}\right) \cdot \left(\frac{T_{\mathrm{f,in}} + T^*_{\mathrm{c,in}}}{2}\right) - T^*_{\mathrm{c,in}}}\right) \tag{4}$$

2. DCMD balancing theory

The balancing framework presented here is based on the analogy between MD systems and heat exchangers presented by Swaminathan et al. [10]. For a counter-flow heat exchanger, the balanced condition corresponds to a case of equal heat capacity rates ($\dot{m}c_{\mathrm{p}}$) of the two streams.

In the case of the MD system, the mass flow rates of the two streams also vary along the length of the channel. For a counterflow MD system though, there is an interesting property that if the feed flow rates of the two streams are equal at any point along the length of the module, they would remain equal at all points along the module.

In countercurrent configuration, the feed flow rate reduces from $x = 0 \to L$, whereas the pure water flow increases from $x = L \to 0$ where $x = 0$ and $x = L$ correspond to feed inlet and outlet, respectively. Since any mass that leaves the feed enters the pure water stream, if the cold water input flow rate is set equal to the flow rate of the feed exit, at every point along the module length, the two flow rates would remain equal. For example, if the feed flow rate and the distillate flow rate are equal at the cold end of the module:

$$\dot{m}_{\mathrm{f,out}} = \dot{m}_{\mathrm{c,in}} \tag{5}$$

The flow rates of the two streams at the other end of the module can be expressed as a function of the pure water produced within the module as:

$$\dot{m}_{\mathrm{f,out}} = \dot{m}_{\mathrm{f,in}} - \dot{m}_{\mathrm{p}} \tag{6}$$

$$\dot{m}_{\mathrm{c,in}} = \dot{m}_{\mathrm{c,out}} - \dot{m}_{\mathrm{p}} \tag{7}$$

and hence $\dot{m}_{\mathrm{f,in}} = \dot{m}_{\mathrm{c,out}}$.

In the case of pure water as the feed, the balanced condition for DCMD systems is particularly simple; the flow rates of the hot and cold streams are equal because the specific heat capacities are identical. Since the flow rate of each stream varies along the length direction, we would set the flow rates at one end of the modules to be equal and hence they remain equal at every point along the length of the module. In addition, in this balanced condition, the flow rates through the external HX are also equal and so the HX is also balanced at the same condition.

2.1. Effect of solutes

For desalination, we are interested in salt water which has different a specific heat capacity compared to that of pure water. As a result, balanced condition for salt water corresponds to a more general case where heat capacity rates (i.e., $\dot{m}c_{\mathrm{p}}$) of the two streams at one end of the system are equal rather than the flow rates. The control system proposed in this study would set the product of the mass flow rate and the specific heat capacity of the cold stream at its inlet to be equal to the product of the mass flow rate and specific heat capacity of the salt water exiting the module:

$$\dot{m}_{\mathrm{c,in}} = \dot{m}_{\mathrm{f,out}} \times \frac{c_{\mathrm{p}}^{\mathrm{f}}}{c_{\mathrm{p}}^{\mathrm{p}}} \tag{8}$$

This can be achieved by using a simple control system that measures the two flow rates and the feed exit salinity as shown in Fig. 2a. If mass flow rate is directly measured, this measurement may be used directly. If instead, a volumetric flow measurement is implemented, the density of the stream as a function of the measured salinity can be used to evaluate the mass flow rate.

This criterion is general and holds true, irrespective of the membrane permeability, area, or heat transfer coefficients within the channels. This method equates the heat capacity rate ratio (or HCR) of the system to unity at the cold inlet, and we refer to this condition as "Balanced" in Fig. 4,5 and 6. Since the recovery in a single pass of DCMD is only about 6-7% usually, salinity of the brine is close to that of the feed and so $c_{\mathrm{p}}^{\mathrm{f}}$ is approximately equal at both ends of the module.

Note that unlike in the case of pure water, where setting this HCR to 1 at one end of the module results in a value of unity throughout the system, in the case of salt water, since $c_{\mathrm{p}}^{\mathrm{f}}$ is not equal to $c_{\mathrm{p}}^{\mathrm{p}}$, along the module the heat capacity rates of the two streams would not be identically equal. More specifically, the mass flow rate at any location is subtracted or added but HCR involves a ratio (i.e., division). Therefore, it is algebraically not possible to maintain HCR of unity when the c_{p} values of the two streams are different.

Then there exists an optimal heat capacity ratio (HCR) value (defined at the cold inlet) that corresponds to a maximum GOR. This condition is referred to as "Max GOR" in Fig. 4,5 and 6. The HCR value corresponding to maximum GOR is determined by numerical optimization in Engineering Equation Solver using a Golden Section search [11] as:

$$\text{Max GOR} = \max_{\text{MR} \in [0.6, 1.4]} \text{GOR} \tag{9}$$

Although the HCR corresponding to this optimal condition is not necessarily unity, we show that "Balanced" condition with HCR = 1 is almost identical to the "Max GOR" case. We will compare the two control systems (Fig. 2) as well as the alternative of setting MR=1.

The comparisons in the subsequent sections are carried out based on the numerical modeling framework described in detail in Summers et al. [2]. The effect of salt concentration polarization is included [8]. The feed stream is assumed to be a sodium chloride solution. The effect of dissolved salt on the vapor pressure of the feed stream is given by:

$$p_{\text{vap}}^{\text{f,m}} = P_{\text{sat}}\left(T_{\text{f,m}}\right) \times a_{\text{w}}\left(T_{\text{f,m}}, s_{\text{f,m}}\right) \tag{10}$$

where a_{w} is the activity of water evaluated using the Pitzer equations as described by Thiel et al. [12].

The effect of salinity on the specific heat capacity of the feed stream is evaluated as a curve fit from the more detailed Pitzer model, at $T = 60\,^{\circ}\text{C}$:

$$c_{\text{p}} = 15.556\, m^2 - 241.78\, m + 4161.9 \tag{11}$$

where c_{p} is the specific heat capacity of the stream in J/kg-K and m is the molality of NaCl.

The baseline parameters for the simulations are given in Table 1.

3. Comparison of various control systems

Figure 2 shows two possible control systems for optimizing the performance of DCMD systems. Note that the balancing method presented in this study, does not involve measuring the top and bottom temperatures reducing the number of measurements required relative to earlier methods. Both these control systems as well as the simple method of setting MR=1 are compared to the numerically evaluated optimal operating condition.

Figure 3 shows that despite not measuring the system top and bottom temperatures, the current balancing method can account for variations in these two parameters. Changes in temperature lead to a change in flux and hence brine mass flow rate which is measured directly. Since mass flow rates are measured, changes in system top temperature can be handled by the proposed control system.

Compared to setting MR=1, GOR is improved significantly by using either of the two control systems (30–60%) (Fig. 4b). At very large lengths, the system based on Eq. 4 deviates from the maximum possible

Table 1: Baseline values for validation test cases

S No	Variable	Value	Units
1	$T_{\mathrm{f,in}}$	85	°C
2	T_{amb}	25	°C
3	$\dot{m}_{\mathrm{f,in}}$	1	kg/s
4	sl_{in}	35	g/kg
5	L	6	m
6	w	12	m
7	$d_{\mathrm{f}}, d_{\mathrm{p}}$	0.001	m
8	B	1.0×10^{-6}	kg/m^2 s Pa
9	$k_{\mathrm{m,material}}$	0.2	W/m K
10	ϕ_{m}	0.8	-
11	δ_{m}	2×10^{-4}	m

GOR, whereas the balancing of the heat capacity rates achieves almost exactly the same result as the numerical optimization.

The reason for the deviation of Lin et al. from the absolute maximum is the fact that heat conduction through the membrane is not accounted for when deriving Eq. 4. At larger module lengths, thermal efficiency (η, which is defined as the fraction of energy transfer across the membrane in the form of mass transfer) is lower since the temperature difference across the membrane is closer to the BPE of the feed stream.

The efficiency η can be expressed as a function of various system parameters [10] as:

$$\eta = \left(1 + \frac{k_{\mathrm{m}}}{\delta_{\mathrm{m}} B h_{\mathrm{fg}}} \frac{1}{bA\mathrm{e}^{bT_{\mathrm{avg}}}\left(1 - \frac{\mathrm{BPE}}{\Delta T_{\mathrm{m}}}\right)}\right)^{-1} \tag{12}$$

where $A = 1054.8$ Pa and $b = 0.0479$ °C^{-1} are fitting parameters based on an exponential curve fit of vapor pressure as a function of temperature ($p_{\mathrm{vap}} = A\mathrm{e}^{bT}$ between 25 °C and 85 °C), T_{avg} is an average temperature within the MD module, BPE is the boiling point elevation at the feed salinity and top temperature, ΔT_{m} is the temperature difference across the membrane, k_{m} is the thermal conductivity of the membrane, and B is the membrane permeability.

In order to illustrate that the present control system performs better at lower values of η, the systems are compared at different values of membrane material conductivity. At larger membrane material conductivity, the thermal efficiency (η) drops. Figure 5 shows that Eq. 4 deviates more from the maximum possible GOR at higher thermal conductivity of the membrane material and lower η.

Figure 6 shows the effect of various control systems over a range of feed salinities. Here as well, at higher

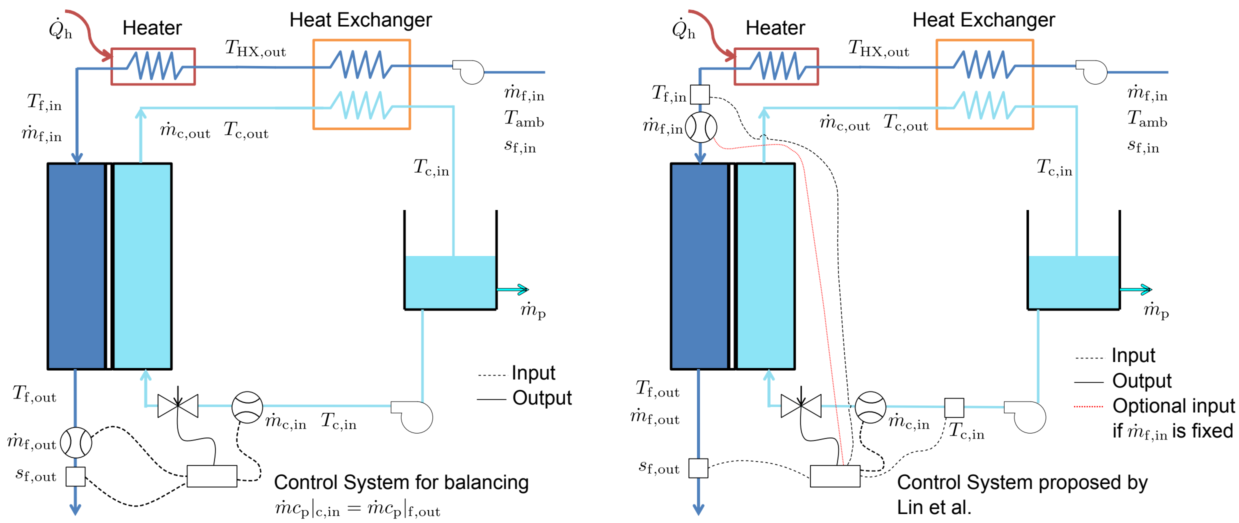

(a) Proposed control system to achieve HCR=1. (b) Control system proposed in Lin et al. (Eq. 4).

Figure 2: Control systems proposed for DCMD GOR balancing.

inlet salinity and correspondingly higher BPE and lower η, a system operating in accordance to , Eq. 4 deviates by up to 15% from the maximum GOR possible. The balancing method proposed in this work does not deviate from the maximum possible GOR until high salinities, and then only by 5%. This deviation is due to the large difference between the specific heat capacities of the two streams.

4. Real-time balancing

Using the proposed control system, dynamic balancing of DCMD can be achieved. This is similar to the dynamic optimization proposed for a humidification dehumidification (HDH) system with changes in operating conditions such as system top and bottom temperatures [13, 14]. The effect of dynamic balancing with changes in system top or bottom temperature is shown in Fig. 7a. Dynamic balancing refers to continuously measuring the flow rates of interest and maintaining a HCR value of 1. This is compared to the case of one-time or initial balancing at $T_{\rm f,in} = 85\,^\circ$C, $T_{\rm c,in} = 25\,^\circ$C and $s_{\rm f,in} = 35$ g/kg, where the HCR is equated to 1 under these operating conditions and the cold stream input flow rate is held constant at this value in spite of changes in system top and bottom temperatures or feed inlet salinity. In HDH, the effective specific heat capacity of the air stream is a non-linear function of temperature due to the exponential dependence of saturation vapor pressure on temperature. As a result, real-time balancing with changing system top or bottom temperature leads to up to 50–150% improvement in GOR.

In MD, real-time balancing has little benefit for changes in system bottom temperature and leads to about 5% increase in GOR for a 40 °C change in system top temperature, compared to initial balancing at the baseline conditions. This difference can be attributed to the higher effect of top temperature on MD performance compared to the bottom temperature due to the exponential nature of vapor pressure

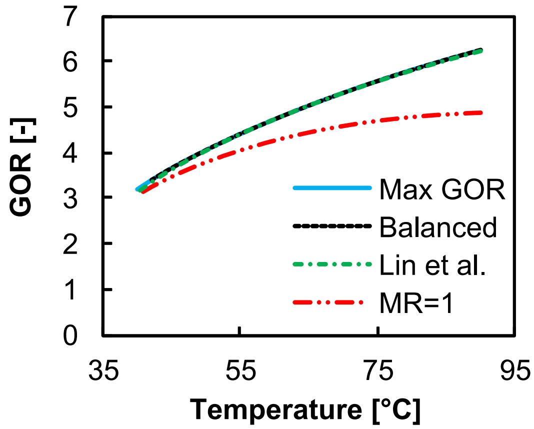

(a) Effect of balancing method on GOR. The curves for "Max GOR", "Balanced" and "Lin et al." coincide.

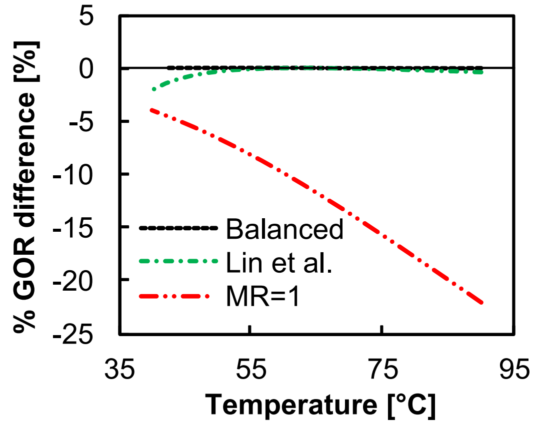

(b) Comparison of GOR from various balancing techniques with maximum GOR possible.

Figure 3: Comparison of balancing techniques at different system top temperature .

dependence on temperature. Since MD performance changes more significantly with top temperature, the effect of balancing is also more for a varying top temperature.

The bottom temperature is varied at a fixed top temperature of 85 °C in this analysis. In real systems, the heat input may be fixed allowing the top temperature to vary with changes in bottom temperature. Under this scenario, the overall effect of changes in bottom temperature could be more significant and real-time balancing may be more useful.

If the incoming feed water salinity was to vary over a wide range ($s_{\mathrm{f,in}} = 35$–200 g/kg), for example in a batch MD process with feed recirculation for achieving higher overall recovery ratio, real-time balancing leads to about 10–15% higher GOR than fixed MR or initial balancing (Fig. 7b), due to the more significant variation in specific heat capacity of water with salinity.

The results presented here do not account for any lag, measurement errors, or other dynamics of the control system. These factors should be considered in more detail when a control system is practically implemented.

5. Conclusions

1. Direct contact membrane distillation can be balanced by setting the heat capacity rate ratio to 1 at one end of the module. Optimization in real-time can be achieved using a simple control system that sets the cold stream inlet flow rate as a function of the feed exit flow rate and salinity as: $\dot{m}_{\mathrm{c,in}} = \dot{m}_{\mathrm{f,out}} \times \frac{c_{\mathrm{p}}^{\mathrm{f}}}{c_{\mathrm{p}}^{\mathrm{p}}}$.
2. Balancing leads to 20-50% higher GOR than a case with equal inlet flow rates.
3. The proposed balancing method results in a GOR very close to that of the absolute maximum GOR achievable, evaluated using numerical optimization. The GOR achieved by the proposed balancing

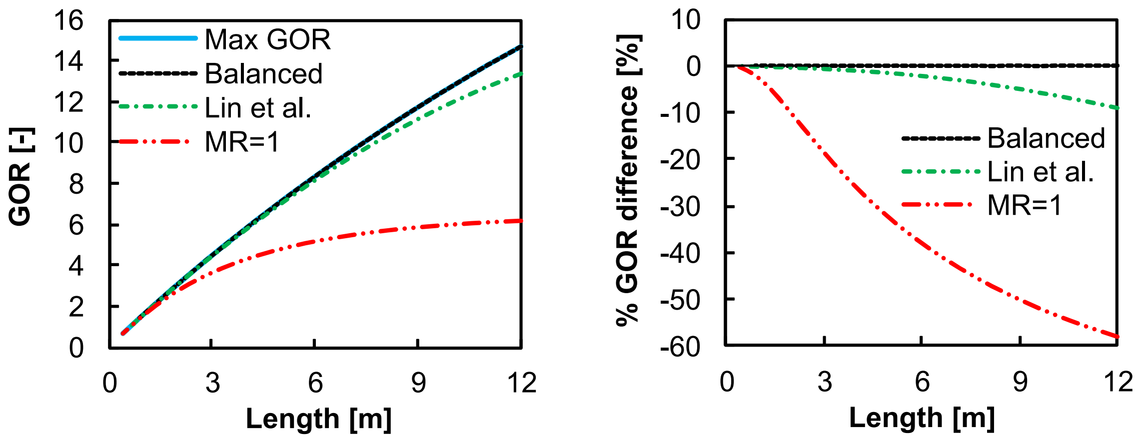

(a) Effect of balancing method on GOR. The curves for "Max GOR" and "Balanced" coincide.

(b) Comparison of GOR from various balancing techniques with maximum GOR possible.

Figure 4: Comparison of balancing techniques for systems of different sizes.

method deviates from the absolute maximum GOR by about 5% at higher feed salinities due to larger difference between $c_{\mathrm{p}}^{\mathrm{f}}$ and $c_{\mathrm{p}}^{\mathrm{c}}$.

4. Over a wide range of operating conditions, the ideal MR evaluated using the permeate limiting formula proposed by Lin et al. [6] results in a performance close to the absolute maximum value. Using their control system, GOR deviates from the maximum possible GOR for systems with low thermal efficiency. That condition occurs at large module length, higher membrane material thermal conductivity or lower permeability, or higher feed salinity.

5. Real-time balancing is most useful compared to one-time or initial balancing, when there are large variations in the feed salinity such as in the case of a batch recirculation system. It may be useful with large changes in system top temperature but will be relatively unimportant for changes in bottom temperature at fixed top temperature.

Acknowledgments

This work was funded by the Cooperative Agreement Between the Masdar Institute of Science and Technology (Masdar Institute), Abu Dhabi, UAE and the Massachusetts Institute of Technology (MIT), Cambridge, MA, USA, Reference No. 02/MI/MI/CP/11/07633/GEN/G/00, and facilitated by the MIT Deshpande Center for Technological Innovation and the Masdar Institute Center for Innovation and Entrepreneurship (iInnovation).

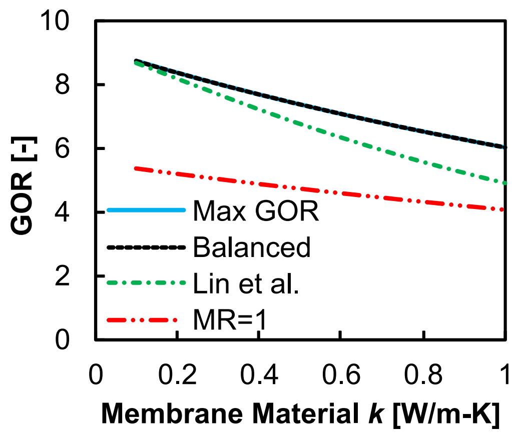

(a) Effect of balancing method on GOR. The curves for "Max GOR" and "Balanced" coincide.

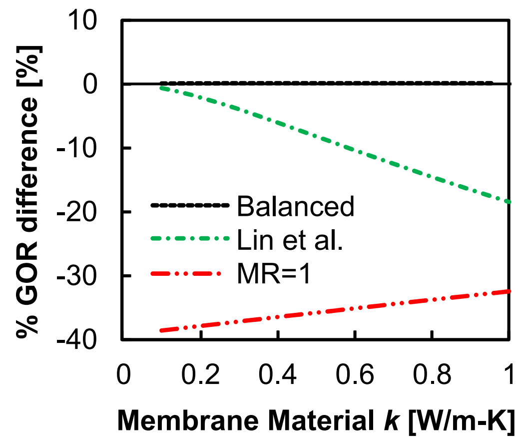

(b) Comparison of GOR from various balancing techniques with maximum GOR possible.

Figure 5: Comparison of balancing techniques at various values of membrane material conductivity.

References

[1] D. M. Warsinger, J. Swaminathan, E. Guillen-Burrieza, H. A. Arafat, J. H. Lienhard V, Scaling and fouling in membrane distillation for desalination applications: A review, Desalination 356 (2014) 294–313. doi:http://dx.doi.org/10.1016/j.desal.2014.06.031.
URL http://www.sciencedirect.com/science/article/pii/S0011916414003634

[2] E. K. Summers, H. A. Arafat, J. H. Lienhard V, Energy efficiency comparison of single-stage membrane distillation (MD) desalination cycles in different configurations, Desalination 290 (2012) 54–66.
URL http://linkinghub.elsevier.com/retrieve/pii/S0011916412000264

[3] R. B. Saffarini, E. K. Summers, H. A. Arafat, J. H. Lienhard V, Economic evaluation of stand-alone solar powered membrane distillation systems, Desalination 299 (2012) 55–62. doi:10.1016/j.desal.2012.05.017.
URL http://www.sciencedirect.com/science/article/pii/S0011916412002779

[4] M. Khayet, T. Matsuura, Membrane Distillation Principles and Applications, Elsevier, 2011.

[5] A. Alklaibi, N. Lior, Membrane-distillation desalination: Status and potential, Desalination 171 (2) (2005) 111–131. doi:10.1016/j.desal.2004.03.024.
URL http://linkinghub.elsevier.com/retrieve/pii/S0011916405800116

[6] S. Lin, N. Y. Yip, M. Elimelech, Direct contact membrane distillation with heat recovery: Thermodynamic insights from module scale modeling, Journal of Membrane Science 453 (2014) 498–515. doi:10.1016/j.memsci.2013.11.016.
URL http://www.sciencedirect.com/science/article/pii/S0376738813009010

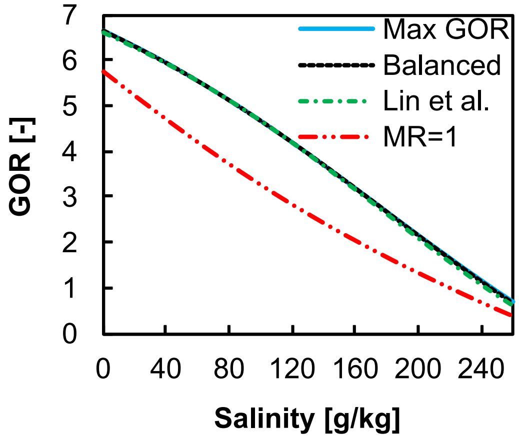

(a) Effect of balancing method on GOR.

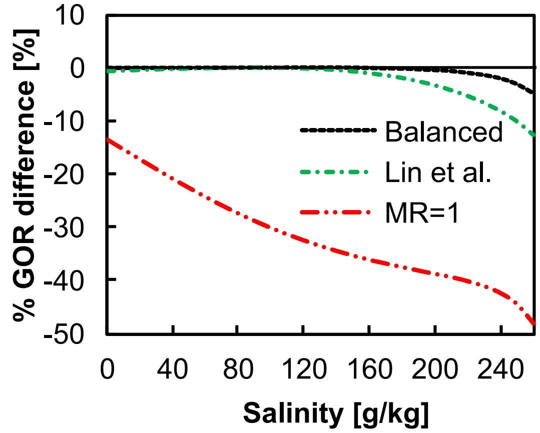

(b) Comparison of GOR from various balancing techniques with maximum GOR possible.

Figure 6: Comparison of balancing techniques with changes in feed salinity.

[7] G. Guan, X. Yang, R. Wang, A. G. Fane, Evaluation of heat utilization in membrane distillation desalination system integrated with heat recovery, Desalination 366 (2015) 80–93. doi:10.1016/j.desal.2015.01.013.
URL http://linkinghub.elsevier.com/retrieve/pii/S0011916415000181

[8] J. Swaminathan, H. W. Chung, D. Warsinger, F. Al-Marzooqi, H. A. Arafat, J. H. Lienhard V, Energy efficiency of permeate gap and novel conductive gap membrane distillation, Journal of Membrane Science 502 (2016) 171–178. doi:10.1016/j.memsci.2015.12.017.
URL http://www.sciencedirect.com/science/article/pii/S0376738815303616

[9] D. Winter, Membrane distillation - a thermodynamic, technological and economic analysis, Ph.D. thesis, University of Kaiserslautern, Germany (2014).

[10] J. Swaminathan, H. W. Chung, D. Warsinger, J. H. Lienhard V, Membrane distillation model based on heat exchanger theory and module comparison, under review (2016).

[11] S.A.Klein, Engineering Equation Solver.
URL http://www.fchart.com/ees/

[12] G. P. Thiel, E. W. Tow, L. D. Banchik, H. W. Chung, J. H. Lienhard V, Energy consumption in desalinating produced water from shale oil and gas extraction, Desalination 366 (2015) 94–112, energy and Desalination. doi:http://dx.doi.org/10.1016/j.desal.2014.12.038.
URL http://www.sciencedirect.com/science/article/pii/S0011916414006857

[13] K. M. Chehayeb, F. K. Cheaib, J. H. Lienhard V, A numerical solution algorithm for a heat and mass transfer model of a desalination system based on packed-bed humidification and bubble column

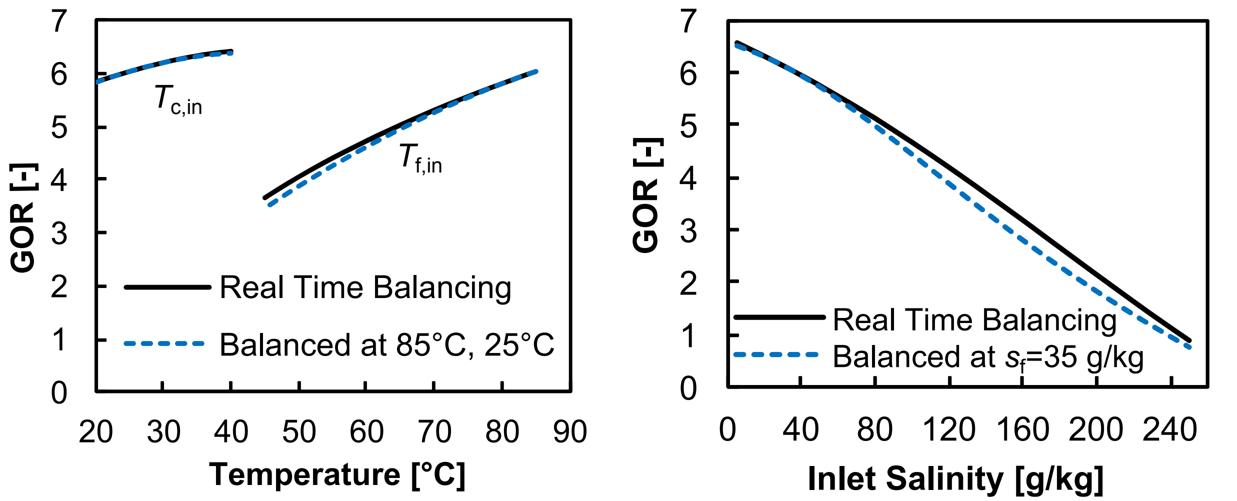

(a) Effect of real-time balancing with changes in system top and bottom temperatures.

(b) Effect of real-time balancing on GOR with changes in inlet salinity.

Figure 7: Effect of dynamic balancing with changes in inlet salinity, top and bottom temperatures.

dehumidification, in: Proceedings of the 15th International Heat Transfer Conference, IHTC-15, Paper No. IHTC15-8995, Kyoto, Japan August 2014.
URL http://web.mit.edu/lienhard/www/papers/conf/IHTC15-8995_Chehayeb.pdf

[14] K. M. Chehayeb, G. P. Narayan, S. M. Zubair, J. H. Lienhard V, Thermodynamic balancing of a fixed-size two-stage humidification dehumidification desalination system, Desalination 369 (2015) 125–139. doi:10.1016/j.desal.2015.04.021.
URL http://www.sciencedirect.com/science/article/pii/S0011916415002660